Hydrophobically Modified Hydroxyethyl Starch: Synthesis, Characterization, and Aqueous Self-Assembly into Nano-Sized Polymeric Micelles and Vesicles

Ahmed Besheer,[†,§] Gerd Hause,[‡] Jörg Kressler,[§] and Karsten Mäder*[,†]

Institute of Pharmaceutical Technology and Biopharmacy, Martin Luther University, Halle-Wittenberg, Wolfgang-Langenbeck-Str. 4, 06120 Halle/Saale, Germany, Microscopy Unit, Biocenter of Martin Luther University, Halle-Wittenberg, Weinberg 22, 06120 Halle/Saale, Germany, and Institute of Physical Chemistry, Martin Luther University, Halle-Wittenberg, 06099, Halle/Saale, Germany

Received October 2, 2006; Revised Manuscript Received November 30, 2006

Hydroxyethyl starch (HES) is a water soluble semisynthetic polysaccharide that is used as a plasma volume expander and cryoprotectant. In order to produce a fully biodegradable amphiphilic polymer, HES was esterified with lauric, palmitic, and stearic acids under mild reaction conditions using dicyclohexyl carbodiimide (DCC) and dimethylaminopyridine (DMAP). The molar substitution of the acyl chains ($MS_{fatty\ acid}$) was determined with ^1H NMR spectroscopy, while the conformational state of the hydrocarbon chains in the graft copolymer was determined using Raman spectroscopy. Furthermore, the aqueous self-assembly of the modified polymer was studied using dynamic light scattering (DLS) and transmission electron microscopy (TEM). Results show the formation of 20 to 30 nm micelles, and 250 to 350 nm polymeric vesicles. Electron spin resonance (ESR) spectroscopy was used to study the microenvironment of a hydrophobic spin probe loaded inside the formed nanodispersion. It was possible to identify the location of the probe and its distribution between the micelles and vesicles. Finally, the hydrophobically modified HES might find use as a potential drug carrier, warranting the future investigation of its ability to encapsulate and deliver drug candidates.

Introduction

Recently, there has been a growing interest in hydrophobically modified derivatives of polysaccharides for biomedical applications. In general, polysaccharides possess a number of favorable characteristics including biotolerability,[1] biodegradability, protein-rejecting ability, receptor interaction through specific sugar moieties, and abundance of functional groups for modification or functionalization.[2] The amphiphilic nature imparted upon polysaccharides after hydrophobic modification gives them a wide and interesting application spectrum, for instance as rheology modifiers, emulsion stabilizers,[3,4] surface modifiers for liposomes and nanoparticles,[4,5] and as drug delivery vehicles.[6,7]

Hydroxyethyl starch (HES) is a semisynthetic polysaccharide obtained by reacting starch with ethylene oxide in alkaline medium. Starch is one of the most abundant polysaccharides in nature.[8] It is usually found as a mixture of two polymers; amylose, a straight chain polyglucan with α-1,4 glycosidic bonds, and amylopectin, the branched variety with α-1,6 bonds for the branch points.[8] HES is usually prepared from starches that are rich in amylopectin such as waxy maize starch and potato starch. The rationale for this selection is that amylopectin is structurally similar to glycogen, the branched glucose storage polymer in humans. This close similarity is believed to be one reason why HES lacks immunogenicity.[9] Furthermore, amylose is responsible for retrogradation and syneresis, which makes amylopectin more favorable to avoid such destabilizing phenomena.[10]

To characterize the substitution of starch with hydroxyethyl units, two terms are used in the literature, namely the degree of substitution ($DS_{hydroxyethyl}$) and the molar substitution ($MS_{hydroxyethyl}$). The definition of these terms in the literature is not unequivocal, and they are often interchanged, leading to confusion.[11−13] In this manuscript, $MS_{hydroxyethyl}$ is defined as the average number of hydroxyethyl groups per anhydroglucose unit (AGU), while $DS_{hydroxyethyl}$ represents the fraction of substituted AGU (regardless whether they have single or multiple substitutions).[12]

Hydroxyethylation imparts a number of desirable properties to starch, namely an increase in solubility and solution stability, and more importantly, an increase in the in vivo half-life.[11,14] The latter is of the order of only a few minutes for native starch due to rapid degradation by serum amylases.[11] On the other hand, the enzymatic biodegradation of HES is hindered due to hydroxyethylation. Accordingly, HES biodegradation depends mainly on the $MS_{hydroxyethyl}$ and the ratio of substitutions to C2 of the AGU relative to that at C6 (C2/C6 ratio), where biodegradation is delayed if $MS_{hydroxyethyl}$ and/or C2/C6 ratio increases. Meanwhile, the molar mass was found to have a negligible influence on biodegradation rate.[15]

From the above explanation, it can be concluded that HES is a water soluble polymer that can be tailored to have the desired physicochemical properties and biodegradation rate. Furthermore, it has a very low risk of hypersensitivity[14] and no drug interactions.[9] Such favorable properties rendered HES as one of the first line colloidal plasma volume expanders (PVEs).[16] Moreover, it is now earnestly investigated as a potential substitute for poly(ethylene glycol) (PEG). The latter is widely

* To whom correspondence should be addressed. E-mail: karsten.maeder@pharmazie.uni-halle.de, phone: +49 345 55-25167, fax: +49 345 55-27029, web: http://pharmtech.pharmazie.uni-halle.de.

† Institute of Pharmaceutical Technology and Biopharmacy, Martin Luther University.

‡ Biocenter of Martin Luther University.

§ Institute of Physical Chemistry, Martin Luther University.

10.1021/bm0609487 CCC: $37.00
Published on Web 01/26/2007

Table 1. Degree of Conversion of the Fatty Acid, Percentage Molar Substitution, and Product Yield As Determined by ^{1}H NMR

sample	HES M_w,[a] 10^3 g/mol	reacting FA[b] (wt in g)	FA:AGU[c]	precipitating solvent	$DC_{fatty\ acid}$,[d] mol %	$MS_{fatty\ acid}$,[e] mol %	yield, %
HES 70-L10.3[f]	70	LA (0.5)	1:3.26	2-propanol/ether 1:1	33.7	10.3	69
HES 200-L8.7	200	LA (0.5)	1:3.26	2-propanol/ether,1:1	28.4	8.7	75
HES 450-L9.4	450	LA (0.5)	1:3.26	2-propanol/ether,1:1	30.6	9.4	76
HES 70-P14.5	70	PA (0.64)	1:3.26	2-propanol/ether 1:1	47.2	14.5	50
HES 200-P16.9	200	PA (0.64)	1:3.26	2-propanol/ether,1:1	55	16.9	65
HES 450-P12.6	450	PA (0.64)	1:3.26	2-propanol/ether,1:1	41.1	12.6	69
HES 70-S7.5	70	SA (0.7)	1:3.26	ethanol/ether,1:1	24.4	7.5	62
HES 200-S5.4	200	SA (0.7)	1:3.26	ethanol/ether,1:1	17.6	5.4	54
HES 450-S4.6	450	SA (0.7)	1:3.26	ethanol/ether,1:1	14.9	4.6	70
HES 70-L19.2	70	LA (1)	1:1.63	acetonitrile/methanol, 1:1	31.3	19.2	67
HES 200-L27	200	LA (1)	1:1.63	acetonitrile/methanol, 1:1	44	27	60
HES 450-L23.3	450	LA (1)	1:1.63	acetonitrile/methanol, 2:1	38	23.3	79

[a] Weight average molar masses are according to the manufacturer. Amount of HES in all reactions was 1.5 g. [b] FA = fatty acid, LA = lauric acid, PA = palmitic acid, SA = stearic acid. [c] Molar ratio, AGU= anhydroglucose unit. [d] $DC_{fatty\ acid}$ = degree of conversion of the fatty acid. [e] $MS_{fatty\ acid}$ = molar substitution of the acyl chains. [f] Sample nomenclature: the numbers 70, 200, 450 refer to the M_W of HES as seen in the second column. The letters L, P, or S refer to the type of fatty acid used as seen in the third column. The number after the letter refers to the molar substitution of the acyl chains as seen in the seventh column.

used to stabilize nanoparticles and liposomes, where it imparts a "stealth" character to them in that they evade (or extend the time before) recognition by the body defense systems.[17,18] Nevertheless, those long-circulating particles are eventually captured by the phagocytic cells and end up in the lysosomes. There, the non-biodegradability and hydrophilicity of PEG can become problematic according to Moghimi and Szebeni who presumed that the inability of PEG to cross the lysosomal membrane can lead to its accumulation there and interference with the lysosomal enzymes.[19] Accordingly, HESylation of proteins instead of PEGylation was proposed[20] and is currently under development. However, using HES to produce stabilized liposomes and nanoparticles has not yet been reported in the literature.

The current paper describes a method for the hydrophobic modification of HES having different molar masses using fatty acids with varying chain lengths. The synthesized graft copolymers were characterized using ^{1}H NMR and Raman spectroscopy, while their aqueous self-assembly behavior was investigated using dynamic light scattering (DLS), transmission electron microscopy (TEM), and electron spin resonance (ESR) spectroscopy.

Materials and Methods

Materials. HES with weight average molar mass (M_w) 70 000, 200 000, and 450 000 g/mol and $MS_{hydroxyethyl}$ 0.5 was a kind gift from Serumwerk Bernburg, Germany. Lauric (C12), palmitic (C16), and stearic (C18) acids as well as dicyclohexyl carbodiimide (DCC) were purchased from Sigma-Aldrich. Dimethylaminopyridine (DMAP) was from Merck, Darmstadt, Germany. 2-Heptadecyl-2,4,5,5-tetramethyl-imidazole-1-oxyl (HD-TMI) was obtained from Prof. V. Khramtsov, Institute of Chemical Kinetics and Combustion, Novosibirsk, Russia. All other chemicals and solvents were reagent grade and used as received, except dimethyl sulfoxide (DMSO) which was stored over 3 Å molecular sieves for drying.

Synthesis. A 1.5 g amount HES was dried at 105 °C for 2 h before dissolving in 20 mL of dry DMSO in a round bottomed flask. To the solution were added the fatty acid, DCC, and DMAP (in the molar ratio 1:1:0.5 respectively), and they dissolved while the flask was tightly sealed and left under stirring at 400 rpm and room temperature (except in case of stearic acid where the temperature was raised to 40 °C) for 24 h. The formed precipitate (dicyclohexyl urea, DCU) was removed by filtration, and the filtrate was added to 200 mL of precipitating solvent mixture (see Table 1). Precipitate was filtered and washed with 100 mL of the same solvent mixture, and then air-dried. The dry polymer was dialyzed against distilled water for 3 days and then lyophilized. Table 1 includes a list of the materials used during synthesis and their amounts.

Nuclear Magnetic Resonance Spectroscopy. For ^{1}H NMR measurements, 30 mg polymer samples were dissolved in 600 μL of d^6-DMSO and measured at 400 MHz (Gemini 2000, Varian Inc.).

Raman Spectroscopy. Raman scattering was recorded at 180° to the incident beam on a Bruker FT-Raman spectrometer RFS 100/S (Bruker Optics, Ettlingen, Germany) using a diode-pumped Nd:YAG laser at an operating wavelength of 1064 nm. The temperature dependence of the Raman spectra of lauric acid was studied in the range from 23 to 55 °C. Temperature variations were performed by flowing tempered air in a glass Dewar cell. After a temperature step, the sample was allowed to equilibrate for 15 min before recording each spectrum. The manipulation and evaluation of the spectra was performed with the Bruker OPUS software.

Preparation of Nanodispersion. A 15 mg amount of polymer was dissolved in 2 mL of a water/THF 1:1 mixture, and then 2 mL of water was added dropwise with stirring. THF was removed by evaporation in a rotary evaporator at 40 °C and 150 mbar. Polymer concentration in the final nanodispersion was 0.5% w/v.

Dynamic Light Scattering (DLS). The hydrodynamic diameter of the particles in the colloidal dispersions was determined by photon correlation spectroscopy at 25 °C, using the back scattering mode (HPPS, Malvern Instruments, UK).

Transmission Electron Microscopy (TEM). For negative staining, the suspension was mixed with 1% aqueous uranyl acetate (1:1). A copper grid coated with Formvar film was placed on a droplet of this mixture for 1 min. Then the liquid was blotted off with filter paper, and the grid was air-dried. The samples were observed with a transmission electron microscope (EM 900, Carl Zeiss SMT, Oberkochen, Germany) operating at 80 kV.

For freeze fracturing, the samples were cryofixed with a propane jet freezer (JFD 60, BAL-TEC, Liechtenstein) and freeze fractured at −110 °C using a BAF 060 freeze fracture apparatus (BAL-TEC, Liechtenstein). After freeze etching for 30 s, the surface was shadowed with platinum (2 nm, shadowing angle 45°) and subsequently with carbon (25 nm, shadowing angle 90°). The replicas were floated in sodium chloride solution (4% Cl) for 30 min, rinsed in distilled water (5 min), and washed in 30% acetone for 30 min. After a final washing in distilled water, the replicas were mounted on grids and observed with a transmission electron microscope (EM 912 OMEGA, Carl Zeiss SMT, Oberkochen, Germany) operating at 80 kV.

Electron Spin Resonance (ESR) Spectroscopy. For ESR measurements, a stock solution of HD-TMI in THF (0.1 mg/mL) was prepared.

Scheme 1. Direct Activation of Fatty Acid with DCC and Subsequent Ester Formation

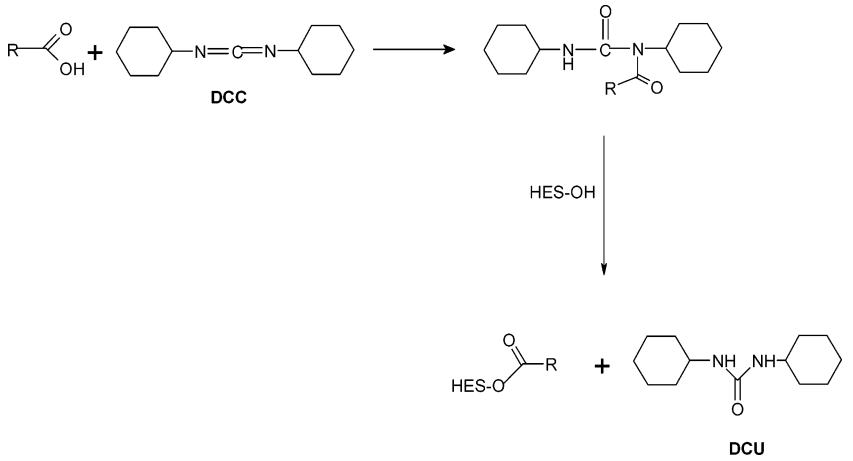

Scheme 2. Activation of Fatty Acid with DCC and DMAP for Ester Formation

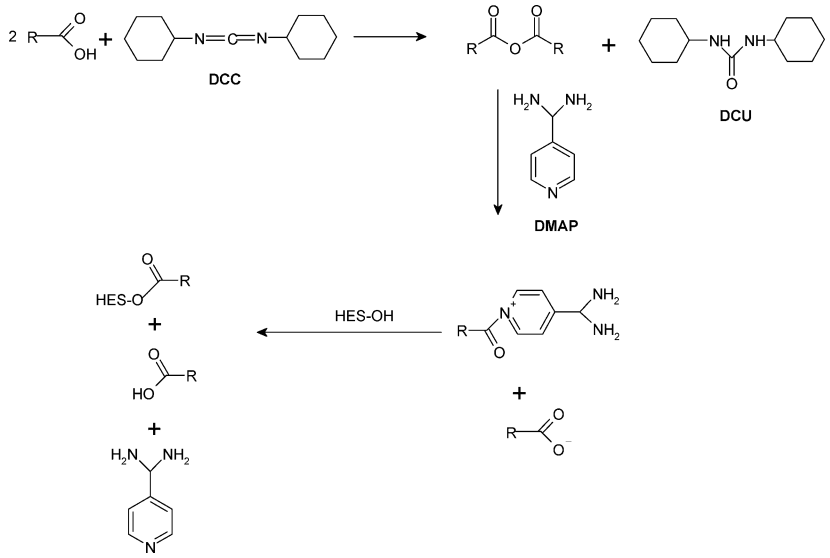

A 15 mg amount of HES 200-L8.7 was dissolved in a mixture of the HD-TMI stock solution (1 mL) and distilled water (1 mL), and then 2 mL of distilled water was added dropwise with stirring. THF was removed using rotary evaporator as mentioned above. The final concentration of HD-TMI was 0.05 mM. Fifty microliter samples were measured in an X-band ESR spectrometer with 9.5 GHz (Miniscope MS 200, Magnettech, Berlin Germany) using the following parameters: Modulation frequency 100 kHz, microwave power 20 mW, scan range 10 mT, scan time 30 s, modulation amplitude 0.1 mT. Spectra were simulated using "nitroxide spectra simulation - v. 4.99" a freeware program developed in the Biophysical Laboratory - EPR center, Josef Stefan Institute, Ljubljana, Slovenia.

Results and Discussion

In general, there are a number of ways to carry out an esterification reaction; however, not all of them are suitable to obtain fatty acid esters of HES. For example, the use of acid chlorides is a simple, effective, and widely spread method to prepare esters; yet HCl, the byproduct of the reaction, can lead to acid hydrolysis of starches.[21] Accordingly, we preferred the use of mild reaction conditions using DCC and DMAP. The mechanism of reaction could be explained by two possible pathways, the first involves direct activation of the fatty acid with DCC followed by reaction with HES hydroxyl groups to form the ester (Scheme 1).[22] In the second pathway, the acid is converted to the anhydride through DCC with the formation of DCU as byproduct. The anhydride reacts with DMAP to form activated acyl pyridinium that then readily esterifies with the hydroxyl groups (Scheme 2).[23] It was necessary to find a solvent for HES and the reactants to carry out a homogeneous reaction, but then the choices were limited, as HES is soluble only in water, DMSO, DMF, and NMP. Water is not suitable for the esterification reaction, and DMSO was chosen, as it has better toxicity profile than DMF and NMP according to the FDA.[24]

A typical ^{1}H NMR spectrum of the modified HES dissolved in d_6-DMSO is shown in Figure 1. Peak assignment for the fatty acid residues was straightforward (see Figure 1 and inset), where the triplet at 0.85 ppm (peak a in Figure 1) belongs to the methyl group of the hydrocarbon chain, the peak at 2.29 ppm (peak d) is related to the methylene group beside the carbonyl group, and the one at 1.5 ppm (peak c) is the methylene group directly before it. All the other methylene groups have a peak at 1.23 ppm (peak b). The clear broadening of the peaks for the methylene groups close to the ester bond (at 2.29 and 1.5 ppm) indicates successful esterification. Meanwhile, peak assignment for HES is not easy due to the overlap between different peaks. By comparing the ^{1}H NMR spectrum for HES with previously published results[25] and with those of amylose and amylopectin,[26,27] it was possible to assign the peaks between 4.4 and 5.7 ppm to four protons, namely the proton bound to C1 of the AGU, and those found in the three hydroxyl groups of the AGU

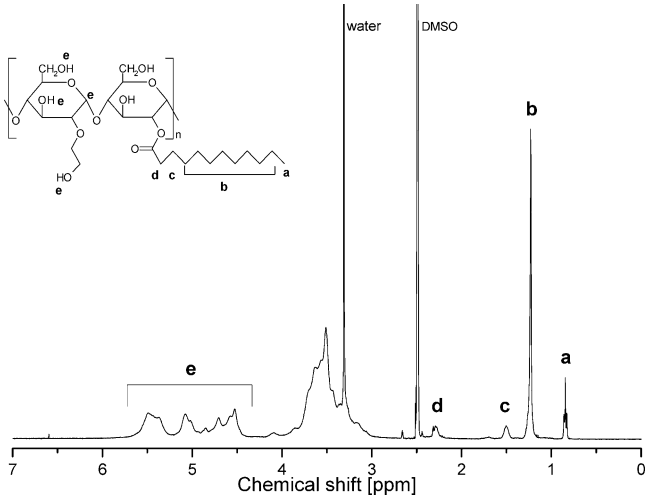

Figure 1. ^{1}H NMR spectrum of HES 200-L8.7. Inset shows the structure of HES laurate and peak assignment.

(regardless whether the OH group is that of glucose or of the attached hydroxyethyl moiety).

^{1}H NMR was used for the calculation of MS of the acyl chains ($MS_{fatty\ acid}$), where it was assumed that each mole of fatty acid removes 1 mol from the protons of the hydroxyl group after esterification. Thus,

$$MS_{fatty\ acid} = \frac{\left(\frac{I_{CH3}}{3}\right)}{\left(\frac{I_{AGU}}{4 - MS}\right)} \quad (1)$$

where I_{CH3} is the integral for the methyl group peak at 0.85 ppm, while I_{AGU} is the integral for the 4 protons of the AGU between 4.4 and 5.7 ppm. Thus ($I_{CH3}/3$) represents 1 mol of the acyl residue, while ($I_{AGU}/4 - MS$) represents 1 mol of AGU after correction, taking into account that the integral area has decreased due to acylation. By rearranging eq 1, $MS_{fatty\ acid}$ can be determined as

$$MS_{fatty\ acid} = \frac{4I_{CH3}}{3I_{AGU} + I_{CH3}} \quad (2)$$

The degree of conversion of the fatty acid ($DC_{fatty\ acid}$) is calculated as

$$DC_{fatty\ acid} = \frac{\text{actual } MS_{fatty\ acid} \text{ determined from NMR}}{\text{nominal } MS_{fatty\ acid}} \quad (3)$$

where the nominal $MS_{fatty\ acid}$ is the expected $MS_{fatty\ acid}$ if all the reacting fatty acid molecules were grafted onto HES.

The yield is calculated as

$$\text{yield} = \frac{\text{mass of modified HES recovered}}{\text{mass of reacting HES} + \text{mass of reacting fatty acid}} \quad (4)$$

Results in Table 1 show that this simple reaction gave satisfactory $DC_{fatty\ acid}$ ranging between 15 and 55 mol % and yields between 50 and 79%. The average $MS_{fatty\ acid}$ (average for the three different molar masses used) increased from lauric acid (9.5 mol %) to palmitic acid (14.7 mol %) despite the same molar ratios of fatty acid to AGU. On the other hand, stearic acid had a much lower average $MS_{fatty\ acid}$ (5.8 mol %). One must note that stearic acid did not dissolve in DMSO at room temperature so that the temperature had to be increased to 40 °C for dissolution. Since many reporters mention the need for relatively low temperature for the reaction of DCC with the acid,[28] the elevated temperature used might have led to this reduction in $MS_{fatty\ acid}$. It is worth mentioning that the polymer molar mass seems to have no effect on the $MS_{fatty\ acid}$, as it is similar for the reactions using the same fatty acid and polymer: fatty acid ratio.

The esterification was further confirmed with Raman spectroscopy (Figures 2 and 3). By comparing the spectra of the modified HES to that of lauric acid and native HES, one can notice the appearance of a shoulder (or a peak for higher $MS_{fatty\ acid}$) at 1440 cm^{-1} due to the CH_2 scissoring and at 1300 cm^{-1} due to CH_2 twisting of the alkyl chains as well as a clear shoulder close to 2852 cm^{-1} due to the symmetric CH_2 stretching of the alkyl chains.

Raman spectroscopy is not only a well-known analytical tool for the identification of functional groups in organic compounds, but it can also deliver information about the conformational state, for instance for hydrocarbon chains.[29] To study this effect, the spectra of crystalline and molten lauric acid at 23 °C and 55 °C, respectively, were compared (N.B., the melting point of lauric acid is 45 °C as confirmed by DSC measurements). The spectrum of lauric acid at 23 °C shows the typical features of well ordered hydrocarbon chains[30,31] (see Table 2 for peak assignment). Upon melting, a number of changes could be observed. Most importantly, the antisymmetric C−H stretching at 2880 cm^{-1}, which is very strong and sharp in the crystalline state, collapses into a broad peak upon melting, while the symmetric C−H stretching peak at 2845 cm^{-1} remains sharp and the peak position increases by 7 cm^{-1}. This latter shift of the symmetric C−H stretching versus temperature was found to be sigmoidal, and the midpoint coincides with the melting temperature (see Figure 4). Furthermore, the decrease in intensity of the C−C stretching peaks at 1063 and 1127 cm^{-1}, and the CH_3 rocking peak at 893 cm^{-1} as well as the disappearance of the splitting of the CH_2 scissoring band at 1400−1480 cm^{-1}, all indicate a loss of order which means an increase of the gauche/trans ratio of the alkyl chains.

To find out the conformational state of the lauryl residues attached to HES, a simulated spectrum was calculated by the addition of spectra of crystalline or molten pure lauric acid, respectively, to that of the unmodified HES 450 (90% of the spectrum was unmodified HES 450 and 10% was pure lauric acid to simulate the $MS_{fatty\ acid}$ of HES 450-L9.4) and then compared to the experimental spectrum. Figure 5 shows the simulated and experimental spectra in the range of CH_2 stretching bands. Obviously, the experimental spectrum does not show the sharp peaks due to the symmetric and antisymmetric stretching modes of the ordered chains, indicating that the acyl chains are indeed in a noncrystalline state. It is worth noting that similar results were found for all types of fatty acids studied and the different polymeric molar masses used.

To study the self-assembly of HM-HES in water, samples were prepared from water/THF solution by gradual addition of water and then evaporation of THF in a rotary evaporator under reduced pressure. Only HES modified with lauric acid and with low $MS_{fatty\ acid}$ (first three polymer samples in Table 1) formed stable nanodispersions, while the others formed a precipitate. These nanodispersions were studied using DLS, TEM, and ESR. The DLS showed two peaks, the first had a z-average size of 20 to 30 nm and is related to polymeric micelles, and the second was between 250 to350 nm and is related to larger aggregates. TEM of negatively stained samples showed a vesicle-like

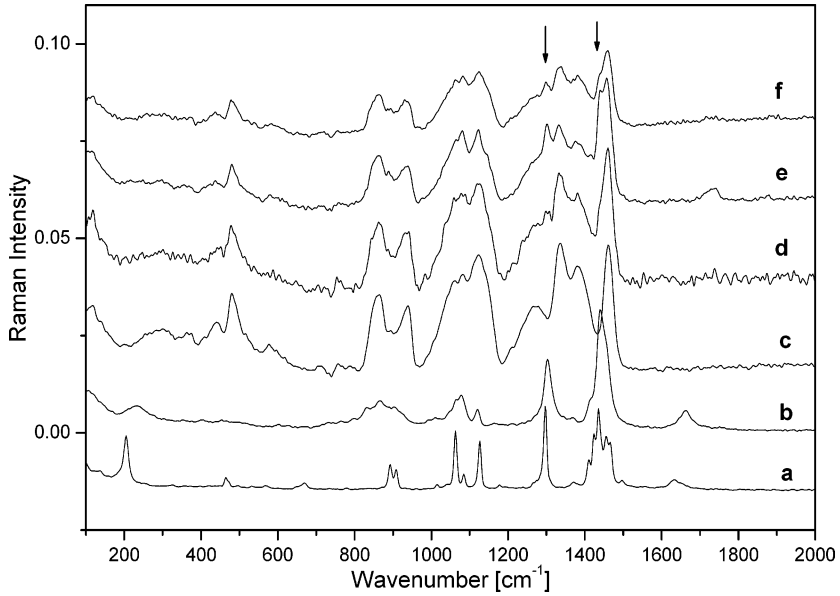

Figure 2. Raman spectra in the range from 100 to 2000 cm^{-1} for (a) lauric acid *studied* at 23 °C, (b) lauric acid at 55 °C, (c) HES 450 (unmodified), (d) HES 450-L9.4, (e) HES 450-L23.3, (f) HES 450-P12.6. Polymer samples were measured at room temperature. The arrow at 1440 cm^{-1} corresponds to the CH_2 scissoring of the fatty acid alkyl chains, while that at 1300 cm^{-1} corresponds to CH_2 twisting of the alkyl chains. See text for discussion.

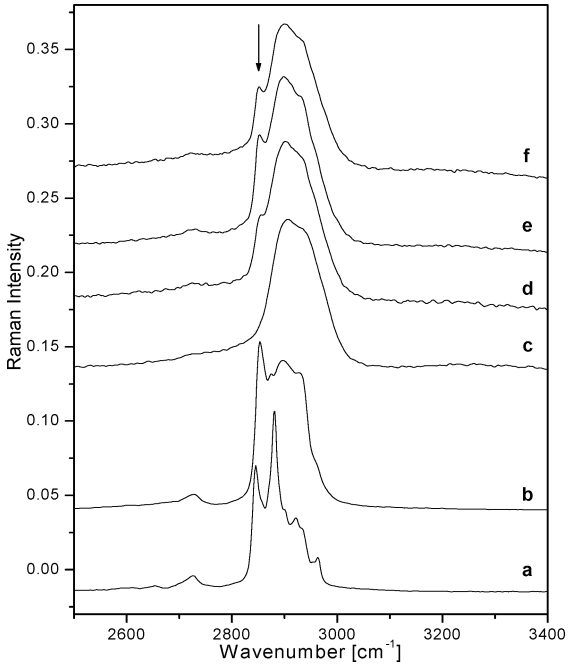

Figure 3. Raman spectra in the range from 2500 to 3400 cm^{-1} for (a) lauric acid measured at 23 °C, (b) lauric acid at 55 °C, (c) HES 450, (d) HES 450-L9.4, (e) HES 450-L23.3, (f) HES 450-P12.6. Polymer samples were measured at room temperature. The arrow at 2852 cm^{-1} is due to the symmetric CH_2 stretching of the alkyl chains of the fatty acid. See text for discussion.

Table 2. Raman Peaks and Their Assignment for Conformationally Sensitive Bands in the Spectrum of Lauric Acid at Room Temperature

peak position (cm^{-1})	assignment
893	CH_3 rocking
1063	C−C antisymmetric stretching for three or more trans−trans bonds in sequence
1127	C−C symmetric stretching for three or more trans−trans bonds in sequence
1297	CH_2 twisting
1410	bending of the CH_2 group adjacent to COOH
1400−1480	CH_2 scissoring
2845	CH_2 symmetric stretching
2880	CH_2 antisymmetric stretching for three or more trans−trans bonds in sequence

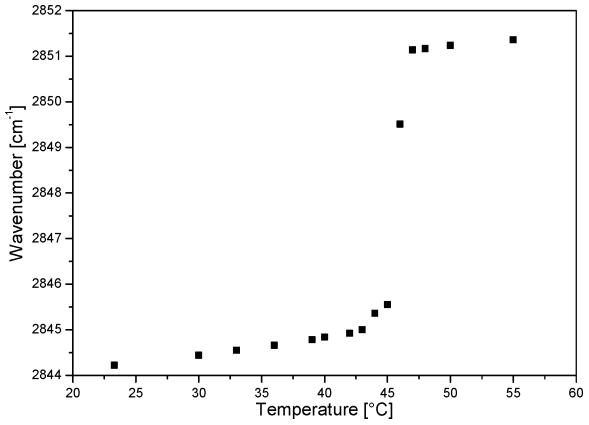

Figure 4. Raman shift of the symmetric CH_2 stretching band of lauric acid as a function of temperature.

structure for the bigger particles. This observation was supported with freeze fracture TEM (Figure 6a and b). In the latter, the vesicles were not intact after fracture, but the fracture plane passed through the vesicles, and one had a cross section in the vesicle that was clear after etching and shadowing (see Figure 6 c). The size of the vesicular structure from freeze-fracture TEM is in the same range of the larger particles from DLS, and the electron micrographs show a broad size distribution.

Ringsdorf et al.[32] have mentioned that hydrophobized polysaccharides cannot self-assemble into vesicles unless there is a hydrophilic spacer molecule between the lipid and the polysaccharide backbone. This is necessary to decouple the movement of the grafted lipid and the stiff backbone; otherwise, a high degree of polymeric cooperativity is needed which makes vesicle-formation very difficult to achieve. The presence of hydroxyethyl units and oligo(ethylene glycol) chains in HES satisfy this necessary prerequisite for such assembly. It is worth

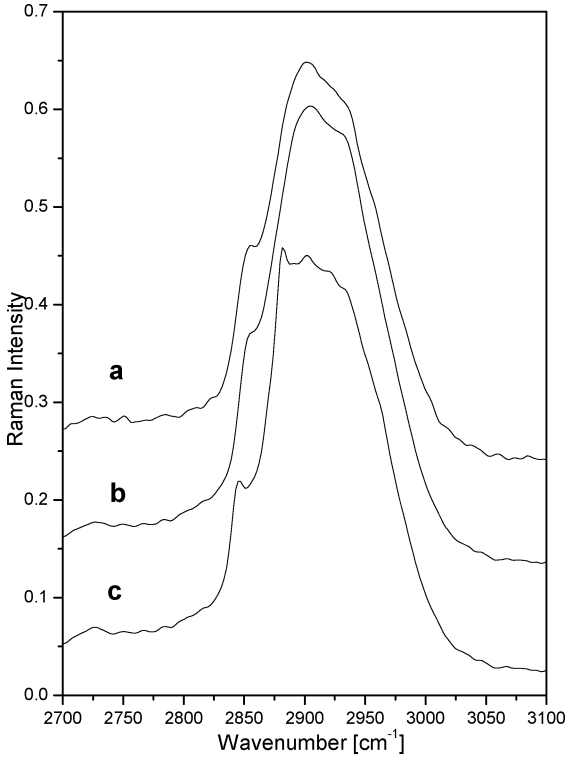

Figure 5. Raman spectra of (a) HES 450-L9.4 at room temperature, (b) sum spectrum consisting of 90% HES 450 and 10% lauric acid at 55 °C, (c) sum spectrum consisting of 90% HES 450 and 10% lauric acid at 23 °C.

mentioning that the formation of vesicles from fatty acid-grafted polysaccharides was reported earlier by Uchegbu et al.,[33,34] where palmitate-modified glycol chitosan self-assembled into vesicular structures in the presence of cholesterol as stabilizer. In general, the interest in polymeric vesicular structures (also known as polymersomes) has increased alot in the past decade from an academic and practical point of view.[35,36] This is because they have an aqueous core which can entrap proteins, polypeptides, or nucleotides,[37,38] and compared to liposomes, they have higher stability, lower membrane fluidity, lower transmembrane permeability, and larger membrane thickness. Most of the studies in this field are on synthetic (usually non-biodegradable) block copolymers,[39] where it is easy to extend the physicochemical formalisms for low molar mass surfactants and polymer physics to the novel vesicles, but few reports deal with vesicles from branched polymers.[40] The expected biotolerability and biodegradability of HM-HES vesicles makes them particularly interesting for further studies on drug/protein encapsulation and possible drug delivery.

ESR spectroscopy is a powerful tool to investigate the local environment of micelles and membranes.[41] It can provide information about the microviscosity, micropolarity, microacidity, and the local oxygen concentration. Accordingly, we used HD-TMI (see structure in inset of Figure 7), a spin probe with a hydrophobic long tail as a reporting molecule, in an attempt to differentiate between the local environment of the vesicles and micelles. Figure 7 shows the spectra of HD-TMI in HES 200-L8.7 nanodispersion, sodium dodecyl sulfate (SDS) micelles, and water, respectively. The spectrum in water shows that the spin probe has precipitated and the very high local concentration leads to spin−spin exchange reflected in the spectrum as one broad peak. On the other hand, the spectrum of HD-TMI in HE 200-L0.5 nanodispersion shows the typical three lines of a tumbling nitroxide; however, the line broadening indicates a relatively viscous environment. This is clear when compared with the spectrum in SDS micelles with little broadening, indicating a fast tumbling and low local viscosity.

The ability of ESR spectroscopy to identify the micropolarity of the spin probe is due to the presence of two resonance structures for nitroxides[42] (Figure 8). Polar solvents stabilize the zwitterionic form of the nitroxide, leading to an increase in the distance between the high and low field lines (this distance is equal to twice the hyperfine splitting constant, $2A_N$).

However, the problem with HD-TMI is that it is not soluble in water, so it is not possible to measure A_N in aqueous media. Knauer and Napier[43] have measured the relation between the hyperfine splitting of three different nitroxides and different solvent polarity parameters. They found out a linear relation ($r^2 = 0.95$) with ET(30), but not with the dielectric constant. (ET(30) is an empirical solvent polarity parameter developed by Dimroth et al.[44,45] This polarity scale is based on the shift of spectrophotometric absorption bands of certain dyes in different solvents as a function of the solvent polarity. The ET(30) values are available for 62 pure solvents and 5 solvent mixtures.[45]) This is because ET(30) represents the solute−solvent interaction at the molecular level while the dielectric constant is a bulk solvent property. This approach can be used to solve the problem of HD-TMI solubility in water, where it allows the construction of a calibration curve and the extrapolation to find A_N of this nitroxide in water. This permits an accurate interpretation of the location of the spin probe inside the nanodispersion.

The relation between the hyperfine splitting and ET(30) for HD-TMI was measured in six different solvents with different polarities (see Figure 9). The relation between ET(30) and A_N was indeed linear with $r^2 = 0.99$. The high correlation is probably due to the small number of solvents used in this study (only 6) compared to 31 solvents used by Knauer and Napier. Yet, it is sufficient to establish the relation and extrapolate to A_N of HD-TMI in water. The latter value was found to be 1.4591 $\pm$ 0.0044 mT. Interestingly, A_N of HD-TMI in SDS solution was found to be 1.4599 mT. The closeness of the latter value to that of HD-TMI in water suggests that the nitroxide is located at the interface. This is in agreement with previous reports that hydrophobic spin probes embedded in SDS micelles have their nitroxide heads located at the interface.[42,46]

When the spectrum of HD-TMI in HM-HES nanodispersion was simulated, the best fit was achieved by using two anisotropic species (Figure 10). Interestingly, A_N of the more predominant species (66%) was equal to 1.4644 mT, indicating the presence of the nitroxide at the interface, while the second species had A_N of 1.4221 mT. The latter value is not similar to that of hexane, as one would expect for a nitroxide that is fully embedded in the fatty acid chains, but it is more to the polar side of the ET(30) scale. An interpretation for the presence of this second nitroxide species with less hydrophilic environment is not trivial. One explanation could be based on the observation of Fukuda et al. who observed a decrease of 0.1 mT in A_N of a hydrophobic spin probe loaded in oleate micelles upon transformation to vesicles.[46] Another explanation can be based on the work of Bales et al.[47] They have found that for SDS micelles loaded with a hydrophobic spin probe, there exists a relation between aggregation number (and accordingly surface curvature or micelle size) and the hyperfine splitting A_N, where A_N decreases as the aggregation number increases. This is because the decrease in surface curvature (or increase in size) leads to decrease in the hydration per unit molecule at the interface, which leads to a decrease in A_N. If one considers the fact that

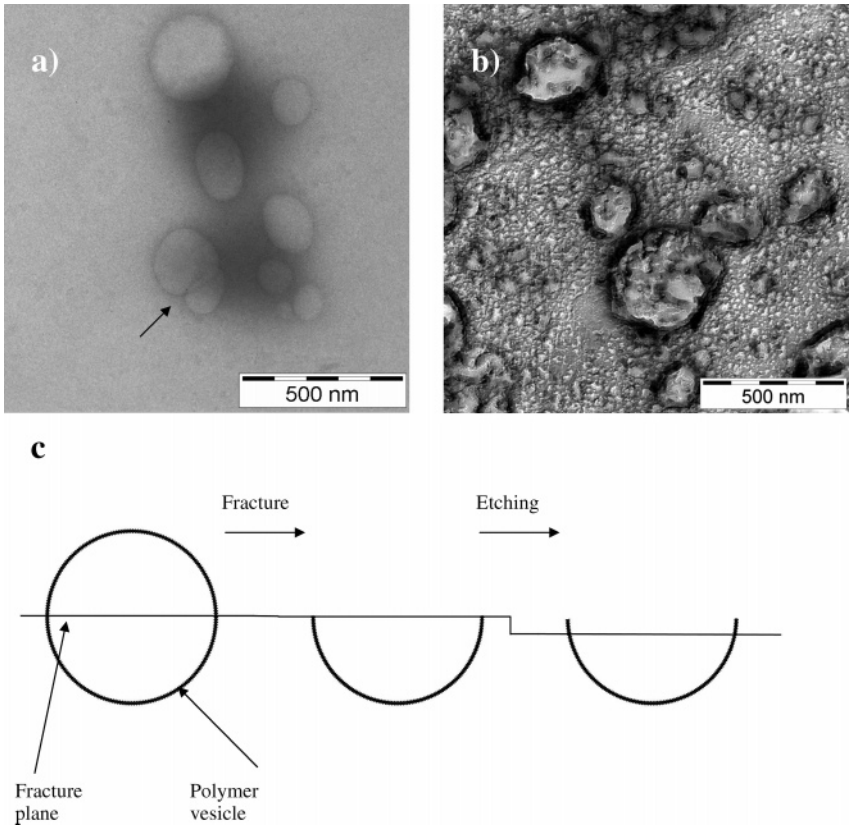

Figure 6. (a) Negative stain TEM micrograph of HES 200-L8.7 nanodispersion (0.5% w/v) showing polymeric vesicles. Arrow points to overlapping vesicles. (b) Freeze fracture micrograph of the same sample c) schematic for the freeze fracture of the polymer vesicle and the etching. The sample is frozen, fractured, and then etched; thus, the walls of the polymeric vesicles are exposed. Shadowing with platinum and carbon provides the necessary contrast for visualization.

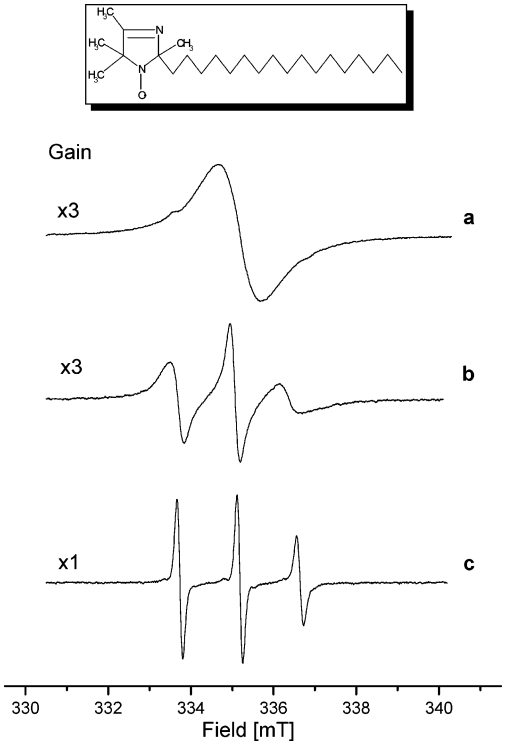

Figure 7. ESR spectra of HD-TMI (a) in water, (b) loaded into HES 200-L8.7 nanodispersion (polymer concn 0.5% w/v), (c) loaded into micellar solution of sodium dodecyl sulfate (surfactant concn 0.5% w/v). Inset shows the structure of HD-TMI.

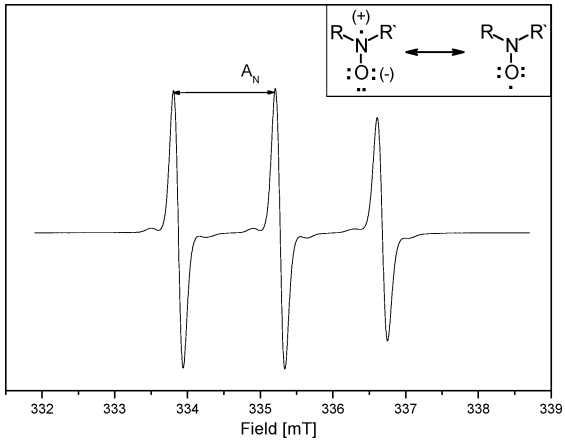

Figure 8. A typical ESR spectrum showing the hyperfine splitting as the distance between the low field peak and the middle peak. Inset shows the two resonance structures of nitroxides, where the polar solvents stabilize the zwitterionic form, leading to an increase of the residence time of the unpaired electron on the nitrogen atom and thus an increase in AN.

the polymeric vesicles are 1 order of magnitude larger in size than the micelles, then it is possible to assign the second minor species (34%) to the spin probe embedded in vesicles interface, while the predominant species, that is sensing a more polar environment, belongs to the spin probe in micelles.

Finally, the aforementioned locations of the nitroxide explain the large difference in mobility of the spin probe (manifested as clear increase in line width) observed between the HM-HES nanodispersion and the SDS micelles. The presence of the nitroxide between the rather stiff polysaccharide chains located at (or near) the interface hinders the mobility of the spin probe and probably favors an axially symmetric rotation of the nitroxide (the fact that the simulated spectra were anisotropic

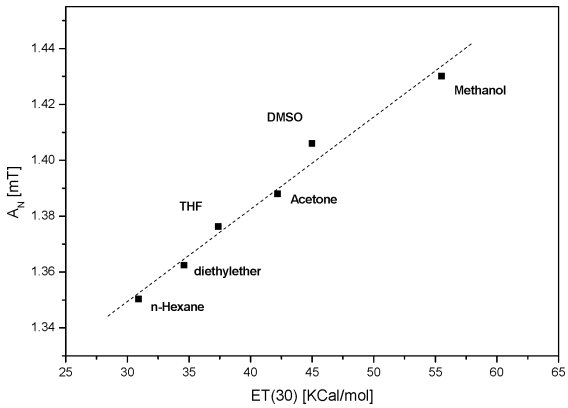

Figure 9. Hyperfine splitting (A_N) of HD-TMI vs ET(30) for 6 different solvents. Dashed line represents the best fit ($A_N = 1.25025 + 0.00331$ ET(30), $r^2 = 0.99$, SD= 0.0044).

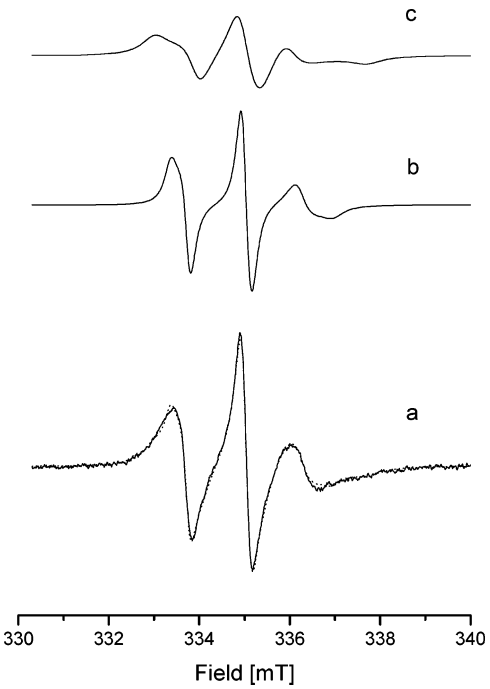

Figure 10. ESR spectra of (a) HD-TMI in HES 200-L8.7 nanodispersion in water (solid line) and the overlaying best fit (dotted line), (b) the first simulated species (66%), and (c) the second simulated species (34%).

favor this postulation). On the other hand, the small ionized sulfate heads of the SDS molecules do not represent such a hindrance to the nitroxide mobility.

Conclusions

HES was hydrophobically modified with lauric, palmitic, and stearic acids by mild esterification using DCC and DMAP. The molar substitution of the acyl chains ($MS_{fatty\ acid}$) was determined using ^{1}H NMR. An average $MS_{fatty\ acid}$ of 9.5 mol % and 14.7 mol % were obtained for lauric and palmitic acid respectively, while stearic acid showed a lower $MS_{fatty\ acid}$ (5.8 mol %). Raman spectroscopy confirmed the esterification and showed that the hydrocarbon chains lost their ability to crystallize after esterification. The aqueous self-assembly of the modified HES was studied after solvent precipitation where only samples modified with lauric acid having $MS_{fatty\ acid}$ between 8.7 and 10.3 mol % formed stable nanodispersions. DLS and TEM showed the formation of micelles and vesicles with z-average size between 20 and 30 nm for the micelles, and 250 to 350 nm for the vesicles. Using a hydrophobic spin probe and ESR spectroscopy, it was possible to identify the location of the probe and its distribution between polymeric micelles and vesicles. The hydrophobically modified HES is indeed interesting for biomedical applications, and its ability to encapsulate and deliver drug candidates will be investigated.

Acknowledgment. A.B. is grateful to the "Excellenzcluster-Nanostrukturierte Materialien", Sachsen-Anhalt for financial support. The authors would like to thank Prof. Dr. S. Wartewig for useful discussions regarding Raman spectroscopy. Serumwerk Bernburg is specially acknowledged for providing the HES samples.

References and Notes

(1) Originally we used the term "biocompatibility". It was the reviewers' opinion that the term "biocompatibility" is mistakenly used in the literature because many "biocompatible" materials, including PEG, do evoke immune responses. We totally agree with the reviewers, and thus we introduced the term "biotolerability" to indicate that although many biomaterials can induce biological responses, they are tolerated by the body.
(2) Lemarchand, C.; Gref, R.; Couvreur, P. *Eur. J. Pharm. Biopharm.* **2004**, *58*, 327−341.
(3) Chen, X. G.; Lee, C. M.; Park, H. J. *J. Agric. Food Chem.* **2003**, *51*, 3135−3139.
(4) Rouzes, C.; Durand, A.; Leonard, M.; Dellacherie, E. *J. Colloids Interface Sci.* **2002**, *253*, 217−223.
(5) Sihorkar, V.; Vyas, S. P. *J. Pharm. Pharm. Sci.* **2001**, *4*, 138−158.
(6) Rodriques, J. S.; Santos-Maqalhaes, N. S.; Coelho, L. C.; Couvreur, P.; Ponchel, G.; Gref, R. *J. Controlled Release* **2003**, *92*, 103−112.
(7) Rouzes, C.; Leonard, M.; Durand, A.; Dellacherie E. *Colloids Surf. B Biointerfaces* 2003, *32*, 125−135.
(8) Ellis, R. P.; Cochrane, M. P.; Dale, M. F. B.; Duffus, C. M.; Lynn, A.; Morrison, I. M.; Prentice, R. D. M.; Swanston, J. S.; Tiller, S. A. *J. Sci. Food Agric.* **1998**, *77*, 289−311.
(9) Brecher, M. E.; Owen, H. G.; Bandarenko, N. *J. Clin. Apheresis* **1997**, *12*, 146−153.
(10) Gosch, C. I.; Haase, T.; Wolf, B. A.; Kulicke, W. *Starch* **2002**, *54*, 375−384.
(11) Dellacherie, E. In *Polysaccharides in medicinal applications*; Dumitriu, S., Ed.; Marcel Dekker: New York, 1996.
(12) Sommermeyer, K.; Hildebrand, U.; Cech, F.; Pfitzer, E.; Henning, K.; Weidler, B. *Starch* **1992**, *44*, 173−179.
(13) *Kolloidaler Volumenersatz aus Bernburg: Infokoll HES 200/0.5 6 % and 10 %*, Product information booklet, Serumwerk: Bernburg, Germany.
(14) Treib, J.; Baron, J.-F.; Grauer, M. T.; Strauss, R. G. *Intensive Care Med.* **1999**, *25*, 258−268.
(15) Jungheinrich, C.; Neff, T. A. *Clin Pharmacokinet.* **2005**, *44*, 681−699.
(16) Schortgen, F.; Deye, N.; Brochard, L. *Intensive Care Med.* **2004**, *30*, 2222−2229.
(17) Gabizon, A. A. *Clin. Cancer Res.* **2001**, *7*, 223−225.
(18) Gref, R.; Domb, A.; Quellec, P.; Blunk, T.; Müller, R. H.; Verbavatz, J. M.; Langer, R. *Adv. Drug Delivery Rev.* **1995**, *16*, 215−233.
(19) Moghimi, S. M.; Szebeni, J. *Prog. Lipid Res.* **2003**, *42*, 463−478.
(20) Orlando, M. Ph.D. Thesis, Universität Giessen, 2003.
(21) Aburto, J.; Alric, I.; Borredon, E. *Starch* **1999**, *51*, 132−135.
(22) Khorana, H. G. *Chem. Rev.* **1953**, 53, 145−164.
(23) Zhang, Z. B.; McCormick, C. L. *J. Appl. Polym. Sci.* **1997**, *66*, 293−305.
(24) FDA, International conference on harmonization; guidance on impurities: residual solvents. *Fed. Regist.* **1997**, 62, 67378. (www.fda.gov/ cder/guidance/1907fnl.pdf).
(25) Lepisto, M.; Artursson, P.; Edman, P.; Laakso, T.; Sjöholm, I. *Anal. Biochem.* **1983**, *133*, 132−135.
(26) Falk, H.; Stanek, M. *Monatsh. Chem.* **1997**, *128*, 777−784.
(27) Wesslen, K. B.; Wesslen, B. *Carbohydrate Polym.* **2002**, *47*, 303−311.
(28) Arai, K.; Shitara, Y.; Ohyama, T. *J. Mater. Chem.* **1996**, *6*, 11−14.
(29) Wartewig, S.; Neubert, R. H.; *Adv. Drug Delivery Rev.* **2005**, *57*, 1144−1170.
(30) Abbate, S.; Zerb, G.i; Wunder, S. L. *J. Phys. Chem.* **1982**, *86*, 3140−3149.

(31) Zerb, G.i; Conti, G.; Minoni, G.; Pison, S.; Bigotto, A. *J. Phys. Chem.* **1987**, *91*, 2386−2393.
(32) Ringsdorf, H.; Schlarb, B.; Venzmer, J.; *Angew. Chem. Int. Ed. Engl.* **1988**, 27, 113−158.
(33) Uchegbu, I. F.; Schätzlein, A. G.; Tetley, L.; Gray, A. I.; Sludden, J.; Siddique, S.; Mosha, E. *J. Pharm. Pharmacol.* **1998**, *50*, 453−458.
(34) Wang, W.; McConaghy, A. M.; Tetley, L.; Uchegbu, I. F. *Langmuir* **2001**, *17*, 631−636.
(35) Discher, D. E.; Eisenberg, A. *Science* **2002**, *297*, 967−973.
(36) Antonietti, M.; Förster, S. *Adv. Mater.* **2003**, *15*, 1323−1333.
(37) Lee, J. C.-M.; Bermudez, H.; Discher, B. M.; Sheehan, M. A.; Won, Y.; Bates, F S.; Discher, D. E. *Biotechnol. Bioeng.* **2001**, *73*, 135−145.
(38) Arifin, D. R.; Palmer, A. F. *Biomacromolecules* **2005**, *6*, 2172−2181.
(39) Discher, B. M.; Won, Y.; Ege, D. S.; Lee, J. C.-M.; Bates, F. S.; Discher, D. E.; Hammer, D. A. *Science* **1999**, *284*, 1143−1146.
(40) Zhou, Y.; Yan, D. *Angew. Chem., Int. Ed.* **2004**, *43*, 4896−4899.
(41) Lurie, D.J.; Mäder K. *Adv. Drug Delivery Rev.* **2005**, *57*, 1171−1190.
(42) Persson, K.; Bales, B. L. *J. Chem. Soc., Faraday Trans.* **1995**, *91*, 2863−2870.
(43) Knauer, B. R.; Napier, J. J. *J. Am. Chem. Soc.* **1976**, *98*, 4395−4400.
(44) Reichardt, C. *Angew. Chem., Int. Ed. Engl.* **1965**, *4*, 29−40.
(45) Dimroth, K.; Reichardt, C.; Siepmann, T.; Bohlmann, F. *Justus Liebigs Ann. Chem.* **1963,** *661*, 1−37.
(46) Fukuda, H.; Goto, A.; Yoshioka, H.; Goto, R.; Morigaki, K.; Walde, P. *Langmuir* **2001**, *17*, 4223−4231.
(47) Bales, B. L.; Messina, L.; Vidal, A.; Peric, M.; Nasciemento, O. R. *J. Phys. Chem. B* **1998**, *102*, 10347−10358.

BM0609487